# Fifteen Years of High-Resolution Radio Imaging of Supernova 1987A

B. M. Gaensler<sup>\*,†</sup>, L. Staveley-Smith<sup>\*\*,‡</sup> and R. N. Manchester<sup>†</sup>, M. J. Kesteven, L. Ball and A. K. Tzioumis<sup>§</sup>

\*School of Physics, The University of Sydney, Sydney NSW, Australia †ARC Federation Fellow \*\*School of Physics, The University of Western Australia, Crawley WA, Australia ‡Premier's Fellow in Radio Astronomy §Australia Telescope National Facility, CSIRO, Marsfield NSW, Australia

#### Abstract.

Supernova 1987A in the Large Magellanic Cloud provides a spectacularly detailed view of the aftermath of a core-collapse explosion. The supernova ejecta initially coasted outward at more than 10% of the speed of light, but in 1990 were observed to decelerate rapidly as they began to encounter dense circumstellar material expelled by the progenitor star. The resulting shock has subsequently produced steadily brightening radio synchrotron emission, which is resolved by the Australia Telescope Compact Array (ATCA) into an expanding limb-brightened shell. Here we present 15 years of ATCA imaging of Supernova 1987A, at an effective angular resolution of 0."4. We find that the radio remnant has accelerated in its expansion over this period, from  $\approx 3600$  km s<sup>-1</sup> in 1992 to  $\approx 5200$  km s<sup>-1</sup> at the end of 2006. The published diameters of the evolving X-ray shell have been  $\sim 15\%$  smaller than the corresponding radio values, but a simultaneous Fourier analysis of both radio and X-ray data eliminates this discrepancy, and yields a current diameter for the shell in both wave-bands of  $\approx 1$ ?7. An asymmetric brightness distribution is seen in radio images at all ATCA epochs: the eastern and western rims have higher fluxes than the northern and southern regions, indicating that most of the radio emission comes from the equatorial plane of the system, where the progenitor star's circumstellar wind is thought to be densest. The eastern lobe is brighter than and further from the supernova site than the western lobe, suggesting an additional asymmetry in the initial distribution of supernova ejecta.

Keywords: circumstellar matter — supernova remnants — supernovae: individual (SN 1987A) PACS: 97.10.Me, 97.60.-s, 98.38.Mz, 98.39.Mz, 98.56.Si

# INTRODUCTION

Supernova (SN) 1987A continues to be an amazing laboratory for studying the interaction between the circumstellar medium (CSM) of a massive star and the subsequent SN ejecta. While the nature of the progenitor star of SN 1987A is still not completely clear [1, 2], a reasonable consensus is that late in its life, Sk  $-69^{\circ}202$  was a red supergiant (RSG), and produced a dense, slow, wind focused into the equatorial plane of the system. About 20 000 years before core-collapse, the star evolved into a blue supergiant (BSG), and began to produce a high-velocity, low density, isotropic wind. The interaction between the BSG and RSG stellar winds, combined with the photo-ionization of the RSG wind by UV photons produced by the BSG, produced the optical "triple-ring" structure seen after the SN (e.g., [3]). The subsequent radio emission produced by the interaction of the expanding ejecta with the swept-up CSM needs to be interpreted within

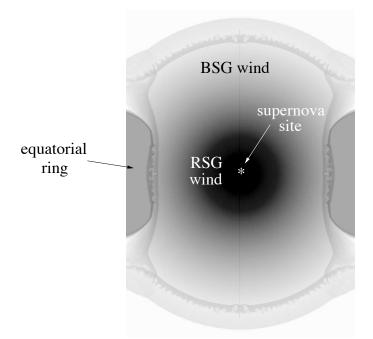


**FIGURE 1.** Hydrodynamic simulation of the CSM around SN 1987A, adapted from [4]. The greyscale represents density, and the system is viewed from the side, such that the equatorial ring is seen edge-on and the nebular symmetry axis is oriented vertically.

the context of this complex pre-existing set of structures (see Fig. 1).

An initial burst of radio emission from SN 1987A was seen by the Molonglo Observatory Synthesis Telescope (MOST) at an observing frequency of 843 MHz, just two days after core-collapse [5]. At this very early stage the radio light-curve was still rising; the flux peaked on day 4, and then exhibited a power-law decay, fading below the detection threshold by day 150. This prompt phase of emission has been interpreted as synchrotron emission produced as the shock moved through the inner regions of the CSM, the swift decay of the flux resulting from rapid motion of the SN shock through the  $\rho \propto r^{-2}$  radial density profile of the BSG stellar wind [6, 7]. At these early epochs, H $\alpha$  and radio VLBI observations both indicate that the shock velocity was  $\approx 19000 - 30000$  km s<sup>-1</sup> [8, 9].

Diligent radio monitoring over subsequent years was rewarded in mid-1990, when the MOST redetected radio emission from SN 1987A. This was quickly followed by confirmation at higher frequencies with the Australia Telescope Compact Array (ATCA). At 9 GHz (the ATCA's highest observing frequency at that time), a diffraction-limited angular resolution of  $\approx 0.0^{\prime\prime}$ 9 could be reached. Such data demonstrated that the new radio source was spatially extended, presumably tracing the interaction between the expanding shock and the swept-up CSM [10, 11]. Here we provide an update on our on-going ATCA imaging campaign (see previous reports by [12, 13, 14]), and discuss what we have have learned from this unique view of an evolving young supernova remnant. The corresponding evolution of the flux density and spectral index are presented by [15] (see also [13, 16], and references therein).

### EXPANSION OF THE SUPERNOVA REMNANT

Since 1992, a deep 9-GHz ATCA observation of SN 1987A has been carried out approximately every six months. Over most of the ensuing 15 years, the source has been bright enough for phase self-calibration, ensuring that the interferometric visibilities are largely free of the errors and systematic uncertainties associated with poor atmospheric phase stability.

The most robust way to track the expansion of the source as a function of time is not to generate images of the sky, but to fit directly to the correlated data in the u - v plane [18]. In particular, [11] and [12] showed that the expansion velocity of the radio remnant could be quantified by fitting the Fourier transform of a transparent thin spherical shell to each observation. The results of this analysis, as applied to data through to the end of 2006, are shown in Figure 2. At the earliest epochs in this plot, at day ~ 1800, the diameter of the shell in the model fit was  $\approx 1.''3$ . Assuming that this source had expanded from size zero at time zero, this implies a mean expansion speed over the period 1987 to 1990–1991 of ~ 38000 km s<sup>-1</sup> (here and below we assume a distance to SN 1987A).

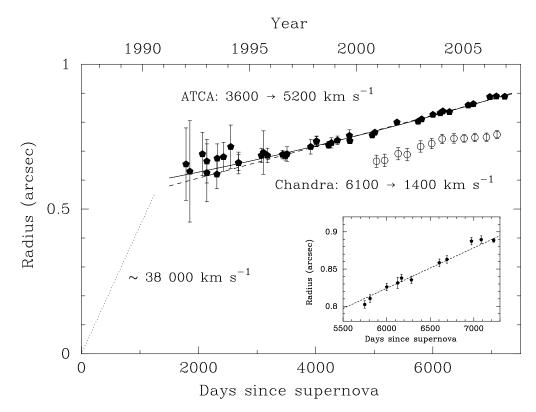


**FIGURE 2.** The expansion of the remnant of SN 1987A. The filled symbols plot the radii inferred from thin spherical shell fits to epochs of 9 GHz u - v ATCA data, while the open symbols plot radii of the shell seen by the *Chandra X-ray Observatory*, as reported by [17]. The dashed line is a linear fit to the radio data, with a slope of  $4700 \pm 100 \text{ km s}^{-1}$ . The solid line shows a quadratic fit, with a slope increasing from  $\approx 3600 \text{ km s}^{-1}$  at day 1800 to  $\approx 5200 \text{ km s}^{-1}$  at day 7200. The dotted line suggests the ballistic expansion of ejecta during the initial period when the remnant was not visible. The inset shows ATCA data over the last 2000 days, with the same linear fit as in the main panel.

of 50 kpc), consistent with essentially free expansion since shock break-out in February 1987.

From day 1800 to day 7200, the source size can be fit well (reduced  $\chi^2$  of 0.74) by constant expansion with a velocity of  $4700 \pm 100$  km s<sup>-1</sup>, shown as a dashed line in Figure 2. Clearly this implies a dramatic deceleration of the ejecta at around the time that radio emission was re-detected in 1990, confirming that the re-emergence of the radio source was due to the shock running into a new high-density zone in the CSM [19, 20].

A slightly better fit to the radio radii is obtained if an acceleration is included, as shown by the quadratic fit (solid line) in Figure 2, which has a reduced  $\chi^2$  of 0.65. For this curve, the expansion velocity increases from  $\approx 3600$  km s<sup>-1</sup> in 1992 to  $\approx 5200$  km s<sup>-1</sup> at the end of 2006. Conversely, the inset to Figure 2 demonstrates that the last three data-points (covering days 6950 to 7250) suggest a possible *deceleration*: a linear fit to these three observations alone gives a velocity of  $200 \pm 1800$  km s<sup>-1</sup>,

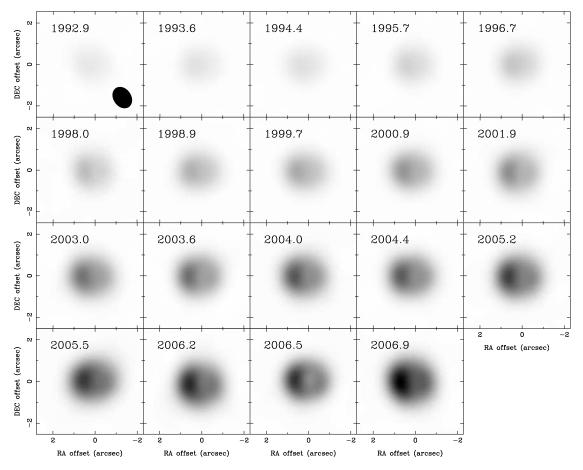


**FIGURE 3.** 9 GHz diffraction limited images of SN 1987A over 14 years of ATCA observations. Each panel is labeled with its corresponding epoch; the same linear greyscale range, between -0.2 and +30 mJy beam<sup>-1</sup>, is used in each panel. The synthesized beam varies slightly between epochs, but typically is an elliptical gaussian of FWHM 0."9 (the beam for the first epoch is shown as an ellipse in that panel).

which is  $\approx 2.5\sigma$  slower than the expansion rate at preceding epochs. In these most recent observations, the radio shell has now reached the same diameter as the equatorial circumstellar ring seen in optical images.

All of this is sharply discrepant to what has been reported for *Chandra X-ray Observatory* data on SN 1987A, taken at comparable angular resolution. The radius of the X-ray shell as reported by [21, 22, 23] is generally  $\sim 15\%$  smaller than what we obtain by fitting to the radio data at similar epochs, while the corresponding X-ray expansion speed was reported to be 6100 km s<sup>-1</sup> before day 6100, dropping to  $\sim 1400$  km s<sup>-1</sup> at later times [17].

# IMAGING, SUPER-RESOLUTION AND SPATIAL MODELING

Although fits to the u - v data give robust measurements and uncertainties, they are less well-suited to dealing with complex morphologies. To move beyond simple spherical shells, we have thus also imaged the 9 GHz ATCA at each epoch. While the diffraction-

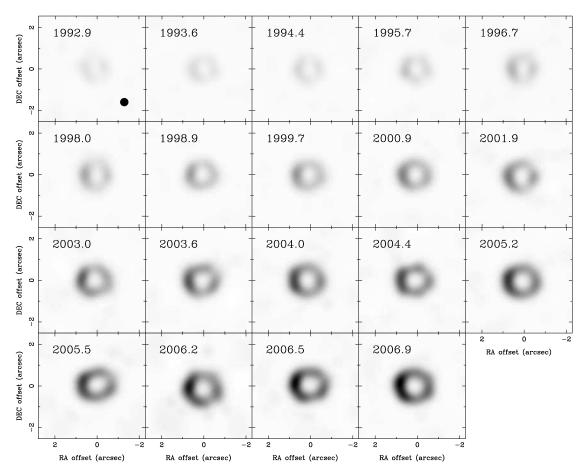


**FIGURE 4.** As in Fig. 3, but after super-resolution has been applied to data at each epoch. The greyscale now ranges from -0.2 to +9.8 mJy beam<sup>-1</sup>, and the synthesized beam for all epochs is a circular gaussian of FWHM 0."4 (as indicated in the first panel).

limited data shown in Figure 3 provide only crude morphological information, application of super-resolution (see [24]), as shown in Figure 4, reveals an approximately circular, limb-brightened shell, dominated by bright lobes to the east and west. The eastern lobe is brighter than the western lobe, and has been brightening more rapidly.

A more quantitative analysis requires a return to the u - v plane. As shown in Figure 5, the thin spherical shell analysis applied in Figure 2 is not an ideal fit to the data. It is thus reasonable to explore the possibility that other simple models might provide a better fit.

A comparison of four spherically symmetric models is shown in the left panel of Figure 6, where we consider fits to the u - v data of a thin spherical shell, a thick spherical shell, a thin circular face-on ring and a thick circular face-on ring. If we try to fit each of these models to the 9-GHz ATCA data, the angular resolution of which is set by a maximum projected baseline of  $\approx 170000$  wavelengths, we can rule out a thin face-on ring, but a thin shell, thick shell and thick face-on ring all match the measurements well, and imply comparable radii of  $\approx 0.2^{\circ}$ .

Higher resolution spatial information is available from new ATCA observations at 18 GHz, as reported for epoch 2003.6 by [14], and as shown for epoch 2004.4 in the right panel of Figure 6. These high-frequency data now extend the coverage of interferometer baselines out to  $\approx 360000$  wavelengths, corresponding to a diffraction limited angular resolution of  $\approx 0.5^{\circ}$ . Even for these long baselines, the u - v fits to a thin shell, thick shell or thick face-on ring all fit the data almost equally well, agreeing to within 5%. We thus conclude that amongst spherically symmetric spatial models, a thin shell is indeed a reasonable description of the source morphology.

In an attempt to understand the apparent discrepancy between the reported radii of the radio and X-ray shells (see Fig. 2), we can Fourier transform *Chandra* data from a comparable epoch to provide equivalent sampling of spatial frequencies out to  $\approx 220000$  wavelengths (mid-way between the 9 and 18 GHz ATCA data-sets). As

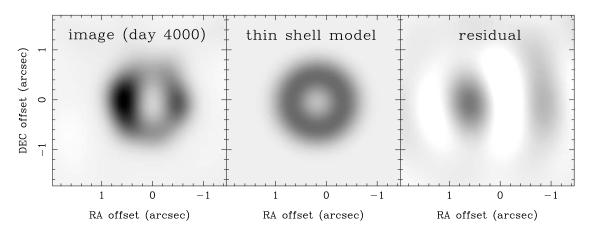


**FIGURE 5.** A fit of a thin spherical shell to the ATCA 9 GHz image of SN 1987A from epoch 1998.0 (see [13] for details). The left panel shows the super-resolved image; the middle panel shows a simulated super-resolved image generated from the complex visibilities of the best-fit thin spherical shell at this epoch; the right panel shows a super-resolved image of the residual visibilities between the data and the model. All three panels are shown on a linear greyscale, ranging between -0.2 and +3.0 mJy beam<sup>-1</sup> at a resolution of 0."4.

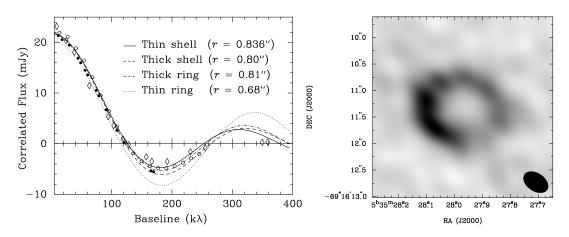
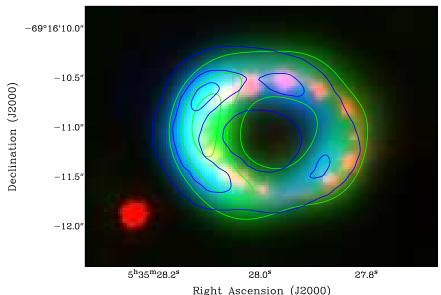


**FIGURE 6.** Left panel: Four different fits to azimuthally averaged u - v data of SN 1987A taken in 2004. The observations shown are 9 GHz ATCA data (solid circles), 1.2–8.0 keV *Chandra* ACIS-S data (open circles) and 18 GHz ATCA data (diamonds). The flux scale corresponds to the 18 GHz ATCA data; the amplitudes of the other two data-sets have been scaled to match this. In all cases the errors in flux are smaller than the plotted points. The curves show the best fits to the 18 GHz data for four different simple models. The best-fit radius, *r*, is indicated in each case. For the thick shell and thick ring, the value shown for *r* corresponds to the outer radius. **Right panel:** Diffraction-limited 18 GHz image of SN 1987A, as seen by the ATCA at epoch 2004.4. The angular resolution is  $0.5^{\prime} \times 0.3^{\prime\prime}$  (as indicated by the ellipse at lower right) and the greyscale is linear over the range -0.5 to +3.1 mJy beam<sup>-1</sup>.

shown in the left panel of Figure 6, the u - v data corresponding to the radio and X-ray observations match to better than 1%, indicating that the published mismatch in source sizes was most likely a result of contrasting measuring techniques, rather than any physical difference.

Interestingly, the dramatic deceleration of the X-ray expansion at around day 6100 reported by [17] is not seen in the radio data (although, as noted above, deceleration of the radio shell may have begun to occur at day  $\sim$  7000). A possible explanation is suggested by the observed decomposition of the X-ray image (e.g., [22]: the soft X-ray image closely traces the optical hot spots seen in the equatorial ring, but in hard X-rays the source shows two opposing lobes that more closely match the radio data (see Fig. 7). The former likely represents relatively slow moving material interacting with dense gas in the equatorial circumstellar ring, while the latter corresponds to higher-velocity ejecta, downstream of the reverse shock, that is yet to experience significant deceleration.

In this case, we interpret the rate of expansion seen for the radio shell as the velocity of the reverse shock before the encounter with the dense equatorial ring. The range of velocities observed in Figure 2 ( $3600-5200 \text{ km s}^{-1}$ ) agrees well with the predictions for this shock velocity of 4100 km s<sup>-1</sup> by [25], and  $3700 \pm 900 \text{ km s}^{-1}$  by [4]. The observed acceleration may be due to increasing amounts of relatively slowly moving SN ejecta catching up with the shock after its initial sudden deceleration in or before 1990. On the other hand, since we are now at the point where the fitted radio radius matches that seen for the surrounding equatorial ring, we now expect to see deceleration in the radio expansion, as may already be beginning to occur.



Right Ascension (00000)

**FIGURE 7.** A multi-wavelength view of SN 1987A. The observations shown are an *HST* WFPC2 F656N image from May 2002 (red image), 1.2–8.0 keV *Chandra* ACIS-S data from July 2005 (green image and green contours) and a 9 GHz ATCA observation from July 2006 (blue image and blue contours). The *HST* and ATCA data are tied to the International Celestial Reference System (see [28]), while the astrometry of the X-ray image is that provided as part of the standard *Chandra* data products.

# MULTI-WAVELENGTH COMPARISONS

A comparison between an *HST* image of the optical ring, a *Chandra* hard X-ray image of shocked gas, and an ATCA radio image of the expanding synchrotron shell is shown in Figure 7. The same two-lobed structure, with brighter regions to the east and west, is seen in both radio and in hard X-rays; a similar morphology can be reconstructed from Ly $\alpha$  and H $\alpha$  spectra of the reverse shock [4, 26, 27].

It seems clear that the two radio lobes are not related to the optical hot spots. The latter are not clustered on the eastern and western parts of the optical ring, and began to appear many years after the radio lobes had already been well-established (see detailed discussion by [13]). The one clear match between the optical and radio data is that the lobes lie along the major axis of the optical ring, suggesting that the true three-dimensional morphology of the radio-emitting region can be approximated as a tilted ring or torus, as shown in Figure 8. This is consistent with the expected distribution of the CSM for Sk  $-69^{\circ}202$ , as discussed earlier: even if the shock driven by the ejecta is close to spherical, the interaction with the CSM should be occurring primarily in the equatorial plane, where the RSG wind is densest. The alignment between the radio lobe orientations and the major axis of the optical ring confirms that the radio emission is indeed dominated by material emitting in the equatorial zones.

Figure 8 also shows what the ATCA would observe for this model, and compares this prediction to the actual data. Apart from the brightness asymmetry between east and west, the match is reasonable. A proper, quantitative comparison in the u - v plane

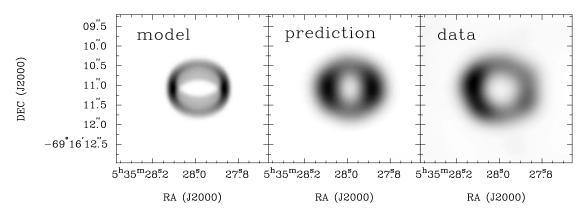


**FIGURE 8.** Comparison of a tilted ring model to radio observations of SN 1987A. The left panel shows an optically thin tilted ring, viewed at an inclination angle of 43°, and with a thickness equal to 25% of its radius. The middle panel shows a simulated ATCA observation of this ring, super-resolved to a resolution of 0."4. The right panel shows a super-resolved 9 GHz ATCA observation of SN 1987A at epoch 2006.9.

requires an analytic expression for the two-dimensional Fourier transform of an optically thin, tilted, three-dimensional ring, and also needs to incorporate the effects of light travel times. We are now in the process of undertaking this more complex analysis.

As noted above, the symmetry is broken by the brightness difference between the two radio lobes. In both the radio and X-ray bands, Figure 7 shows that the brighter eastern lobe is at a larger distance from the explosion site than the western lobe, suggesting an asymmetry in the initial velocity of the ejecta, rather than in the ambient density [12].

# CONCLUSIONS

The turn-on of radio emission from SN 1987A in 1990 and the accompanying sudden drop in the expansion velocity of the ejecta marked the initial encounter between the outward moving supernova debris and the dense red supergiant wind. Over the ensuing years, the radio remnant of SN 1987A has continued to brighten and expand.

A joint analysis of radio and X-ray observations of this source leads to a consistent multi-wavelength picture, in which the reverse shock is the source of both the synchrotron emission seen in the radio band, and of the high-temperature shocked gas seen in hard X-rays. The morphology of this region can be reasonably approximated by a thin spherical shell, currently expanding at  $\sim$ 5200 km s<sup>-1</sup>. The symmetry is broken by the presence of two bright lobes on the eastern and western rims of the radio and X-ray shells, indicating that the shock is predominantly interacting with dense gas in the equatorial plane of the progenitor system. In the near future, we hope to better quantify the geometry of this interaction via Fourier modeling of axisymmetric as well as spherical morphologies.

Clearly the collision of the ejecta piston with dense gas in the optical circumstellar ring is now almost fully upon us. As we watch this spectacular interaction play out over the coming decades, we can look forward to wider frequency coverage and higher resolution images of this remarkable source using forthcoming facilities such as ALMA, MIRANdA and the Square Kilometre Array.

# ACKNOWLEDGMENTS

We thank the organizers and hosts for a very informative and enjoyable workshop, and also thank Sangwook Park and Judy Racusin for providing X-ray data on SN 1987A in advance of publication. The Australia Telescope is funded by the Commonwealth of Australia for operation as a National Facility managed by CSIRO. B.M.G. and R.N.M. acknowledge the support of the Australian Research Council.

# REFERENCES

- 1. T. Morris, and P. Podsiadlowski, *Science* **315**, 1103–1106 (2007).
- 2. N. Smith, AJ 133, 1034–1040 (2007).
- 3. C. J. Burrows et al., *ApJ* **452**, 680–684 (1995).
- 4. E. Michael et al., *ApJ* **593**, 809–830 (2003).
- 5. A. J. Turtle et al., *Nature* **327**, 38–40 (1987).
- 6. M. C. Storey, and R. N. Manchester, *Nature* **329**, 421–423 (1987).
- 7. R. A. Chevalier, and C. Fransson, *Nature* **328**, 44–45 (1987).
- 8. R. W. Hanuschik, and J. Dachs, *A&A* 182, L29–L30 (1987).
- 9. D. L. Jauncey et al., *Nature* **334**, 412–415 (1988).
- 10. L. Staveley-Smith et al., Nature 355, 147–149 (1992).
- 11. L. Staveley-Smith, D. S. Briggs, A. C. H. Rowe, R. N. Manchester, J. E. Reynolds, A. K. Tzioumis, and M. J. Kesteven, *Nature* **366**, 136–138 (1993).
- 12. B. M. Gaensler, R. N. Manchester, L. Staveley-Smith, A. K. Tzioumis, J. E. Reynolds, and M. J. Kesteven, *ApJ* **479**, 845–858 (1997).
- 13. R. N. Manchester et al., Publ. Astron. Soc. Aust. 19, 207-221 (2002).
- 14. R. N. Manchester, B. M. Gaensler, L. Staveley-Smith, M. J. Kesteven, and A. K. Tzioumis, *ApJ* 628, L131–L134 (2005).
- L. Staveley-Smith, B. M. Gaensler, R. N. Manchester, L. Ball, M. J. Kesteven, and A. K. Tzioumis, in Supernova 1987A: Twenty Years After: Supernovae and Gamma-Ray Bursters, edited by S. Immler, K. W. Weiler, and R. McCray, American Institute of Physics, New York, 2007, in press.
- 16. L. Ball, D. F. Crawford, R. W. Hunstead, I. Klamer, and V. J. McIntyre, ApJ 549, 599-607 (2001).
- S. Park, D. N. Burrows, G. P. Garmire, R. McCray, J. L. Racusin, and S. A. Zhekov, in *Supernova* 1987A: Twenty Years After: Supernovae and Gamma-Ray Bursters, edited by S. Immler, K. W. Weiler, and R. McCray, American Institute of Physics, New York, 2007, in press (arXiv:0704.0209).
- 18. L. Staveley-Smith, R. N. Manchester, M. J. Kesteven, A. K. Tzioumis, and J. E. Reynolds, *Publ. Astron. Soc. Aust.* **10**, 331–334 (1993).
- 19. R. A. Chevalier, and V. V. Dwarkadas, *ApJ* **452**, L45–L48 (1995).
- 20. P. Duffy, L. Ball, and J. G. Kirk, ApJ 447, 364–377 (1995).
- S. Park, D. N. Burrows, G. P. Garmire, J. A. Nousek, R. McCray, E. Michael, and S. Zhekov, *ApJ* 567, 314–322 (2002).
- 22. S. Park, S. A. Zhekov, D. N. Burrows, G. P. Garmire, and R. McCray, ApJ 610, 275–284 (2004).
- 23. S. Park, S. A. Zhekov, D. N. Burrows, J. L. Racusin, R. McCray, and K. J. Borkowski, in *The X-ray Universe 2005*, edited by A. Wilson, ESA Publications Division, 2006, pp. 335–340.
- 24. D. S. Briggs, in *The Restoration of HST Images and Spectra II*, edited by R. J. Hanisch, and R. L. White, Space Telescope Science Institute, Baltimore, 1994, pp. 250–256.
- 25. K. J. Borkowski, J. M. Blondin, and R. McCray, ApJ 476, L31–L34 (1997).
- 26. E. Michael et al., *ApJ* **509**, L117–L120 (1998).
- 27. K. Heng et al., ApJ 644, 959-970 (2006).
- 28. J. E. Reynolds et al., *A&A* **304**, 116–120 (1995).